Sediment Dynamics and the Hydromorphology of Fluvial Systems (Proceedings of a symposium held in Dundee, UK, July 2006). IAHS Publ. 306, 2006.

Predicting erosion patterns using a spatially distributed erosion model with spatially variable and uniform parameters

DIRK H. DE BOER

Department of Geography, University of Saskatchewan, 9 Campus Drive, Saskatoon, Saskatchewan S7N 5A5, Canada

deboer@duke.usask.ca

Abstract Distributed models are generally viewed as the best type of model for evaluating the erosional response of a drainage basin to changes in land use, climate, and other controlling factors. In many instances, however, information about the spatial variability of the model parameters is not available so that, even though the model is spatially explicit, parameters are treated as though they were uniform across the basin. The objective of this study was to compare the results of model runs with spatially variable parameters with those of model runs with uniform parameters. The model used is Cascade 6, a grid-based erosion model which requires data on elevation, saturated conductivity, surface roughness, and soil cohesion for each grid cell. The model was applied to the 45-ha Catsop basin located in the province of South-Limburg, The Netherlands. This loess-covered basin has a gently to moderately sloping topography, and land use is predominantly agricultural. The model is calibrated for peak discharge and sediment rating curve, and calibration is carried out separately with spatially variable and uniform runoff and erosion parameters. Model results indicate that erosion rates for individual grid cells modelled with variable parameters can be predicted from the erosion rate modelled with uniform parameters for grid cells with a drainage area from 1 to 1000 grid cells. Thus, the spatial pattern of erosion in the basin can be modelled over 85% of the basin area even in the absence of information about the spatial variability of the runoff and erosion parameters.

Key words distributed model; erosion model; parameterization; sediment

INTRODUCTION

Distributed models are generally viewed as the best type of model for evaluating the erosional response of a drainage basin to changes in land use, climate, and other controlling factors. One of the advantages of this kind of model is that it enables predicting the pattern of erosion and deposition within a drainage basin rather than just providing an estimate of the basin output. This is an important step towards the design of effective erosion control measures, as it allows targeting of the specific areas that are most susceptible to erosion. The use of GIS has been a big step forward in the parameterization of distributed models, as it allows available data on land use, soil type, vegetation and other factors to be used as distributed input data (De Roo, 1998). Jetten *et al*. (2003) view the spatial and temporal variation of input parameters as a fundamental reason for the poor to moderate quality of the predictions of erosion models. In many instances, however, information about the spatial variability of the model parameters is not available so that, even though the model is spatially explicit, parameters are treated by necessity as though they were uniform across the basin. The objective of this study is to compare the results of model runs with spatially variable parameters with those of model runs with uniform parameters.

MODEL DESCRIPTION

The model used for this study is Cascade 6, an event-based erosion model that operates at the drainage-basin scale. It is based on an earlier model, Cascade 5, which was developed to investigate self-organization and emergence in synthetic, erosional landscapes over long timescales (De Boer, 2001; De Boer & Ali, 2002; Favis-Mortlock & De Boer, 2003). Cascade 6 is grid-based, and for each grid cell requires data on elevation, saturated conductivity, surface roughness, and soil cohesion. Cascade 6 uses a time step, with a length in seconds, equal to the grid cell size in metres, i.e. the time step is 10 s for 10 × 10 m grid cells. For each time step, precipitation is added to all grid cells in the basin. It is assumed that all rainfall infiltrates as long as the cumulative infiltration is less than P_{min}, the rainfall threshold which represents the initial loss due to interception, depression storage, and the initially high infiltration capacity of the soil. Once P_{min} is exceeded, the infiltration rate is equal to K_{sat}, and excess water runs off.

Water is routed from a cell to its lowest neighbour using the Manning equation. The flow velocity and depth are used to calculate the discharge from a cell to its lowest neighbour, and the sediment flux is calculated as:

$$Q_s = k\, Q^m S^p \qquad (1)$$

where: Q_s is the sediment flux (kg time step^{-1}), Q is the discharge (m^3 time step^{-1}), S is the slope (elevation difference divided by distance), k is a measure of the soil erodibility in a grid cell, and m and p are constants (Howard, 1994; Dietrich *et al.*, 2003). Following Kirkby (1993), Tucker & Slingerland (1997) and others, it is assumed that the sediment flux varies linearly with S, so that $p = 1$. The relationship between the discharge and the sediment flux, however, is non-linear, and $m > 1$. In Cascade 6, sediment transport is assumed to be transport-limited, i.e. the sediment concentration is controlled by the flow conditions.

FIELD AREA

The 45-ha Catsop basin is located in the province of South-Limburg, The Netherlands (De Roo, 1996). This loess-covered basin has a gently to moderately sloping topography, and land use is predominantly agricultural. Data from the Catsop basin have been used in a variety of earlier modelling exercises, enabling comparison of the Cascade 6 results with those from other models (e.g. De Roo *et al.*, 1996a,b). Data from the Catsop basin were used in the GCTE model comparison exercise (De Roo & Jetten, 1999; Jetten *et al.*, 1999), and a portion of these data was used for the present study.

CALIBRATION

Calibration of Cascade 6 is discussed in detail by De Boer (2005). In brief, Cascade 6 has five parameters that can be adjusted during calibration. Two of these relate directly to runoff generation: the rainfall threshold P_{min} and the saturated conductivity K_{sat}. It is assumed that P_{min} is the same for all cells, regardless of surface characteristics. Conversely, K_{sat} is spatially variable and depends on land use or soil type. During calibration, Cascade 6 uses a K_{sat} calibration factor to change K_{sat} by the same percentage for all cells, thus preserving the spatial pattern in K_{sat}. The K_{sat} calibration factor is varied to adjust the peak (Q_{peak}) discharge, as this was deemed the most important variable for controlling sediment load.

The Manning coefficient is spatially variable in Cascade 6 to reflect, for example, differences in land use or vegetation type. Cascade 6 uses a Manning coefficient calibration factor to vary the Manning coefficients by the same percentage for all cells so that the spatial pattern of surface roughness is retained. The Manning coefficient calibration factor was altered during calibration to adjust the shape of the modelled hydrograph and the timing of Q_{peak}.

During calibration, the sediment transport parameters *m* and *k* are adjusted so that the modelled and observed sediment rating curves match. The same value of *m* is used for all cells. The other parameter, *k*, reflects soil and sediment properties such as erodibility and particle size distribution, and is spatially variable, depending on land use and soil type. For this study, *k* is inversely proportional to the soil cohesion provided in the Catsop data set. A *k* calibration factor is used to reduce or increase *k* by the same percentage for all cells so that the spatial pattern is preserved.

RESULTS AND DISCUSSION

Table 1 shows the observed peak discharge, total discharge and soil loss for the storm event of 26 June 1987, and the model results obtained with spatially variable and uniform parameters. Figure 1 shows the hydrographs for the 26 June 1987 event modelled using spatially variable and uniform parameters. Cascade 6 was calibrated for peak discharge for both model runs. Because the hydrograph peak is broader for the model run with uniform parameters than for the run with the variable parameters, the total discharge is also larger (735 *vs* 487 m^3). A similar difference in magnitude is shown by the soil loss, which is 2253 kg for the model run with uniform parameters

Table 1 Observed values and Cascade 6 model results for the 26 June 1987 event.

Manning factor	*K* factor	*m*	K_{sat} factor	P_{min} (mm)	Q_{peak} (L s^{-1})	Q_{total} (m^3)	Soil loss (kg)	Rating curve coefficient	Rating curve exponent
Observed					226.7	487	1900	0.977	0.248
Variable									
0.08	147	1.246	0.130	2	224.2	487	1410	0.9594	0.2505
Uniform									
0.0155	44	1.24	5.7	2	224.3	735	2253	0.9951	0.244

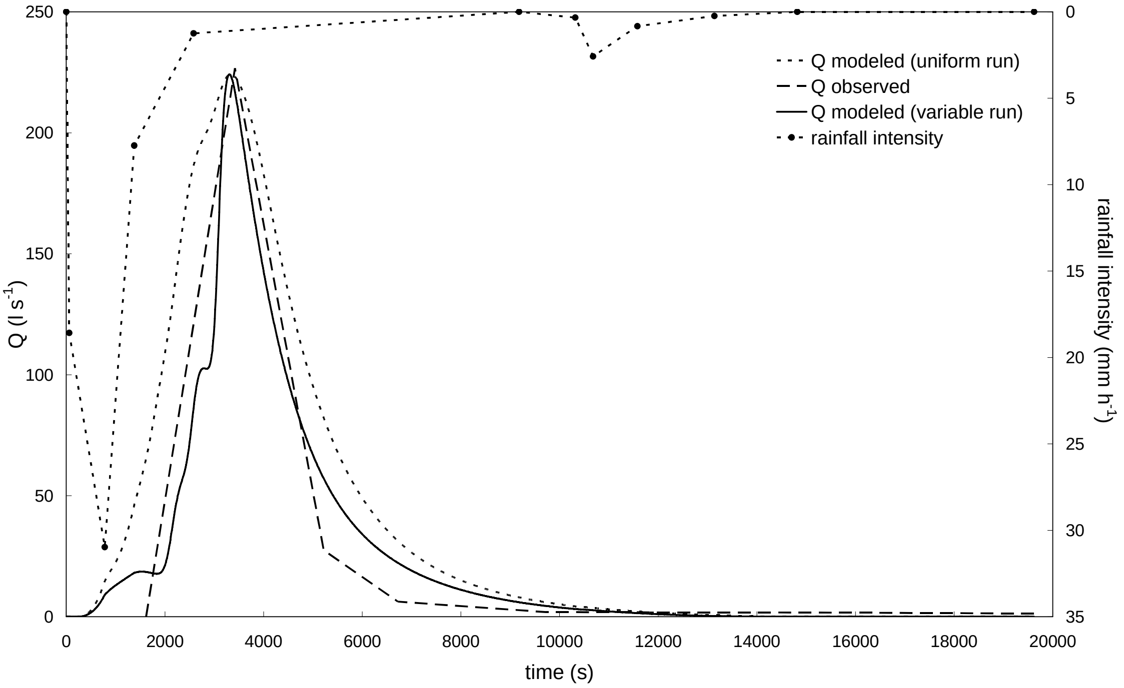

Fig. 1 Observed and modelled hydrographs for the event of 870626 with spatially variable and uniform parameters.

Table 2 Overview of parameter values for various land use classes and uniform conditions used in Cascade 6 for the 26 June 1987 event.

			GCTE data set			Calibrated in Cascade 6		
						Calibration factors:		
Land use						0.08	147	0.13
class	Cells	% Area	Manning's *n*	*k*	K_{sat}	Manning's *n*	*k*	K_{sat}
2	622	15.0	0.259	3.32	52.1	0.021	488.04	6.8
4	1806	43.5	0.14	1	25.3	0.011	147	3.3
5	549	13.2	0.124	0.86	205.1	0.010	126.42	26.7
6	829	19.9	0.144	1.02	205.1	0.012	149.94	26.7
12	178	4.3	0.14	1	25.3	0.011	147	3.3
14	12	0.3	0.124	0.86	205.1	0.010	126.42	26.7
15	160	3.8	0.124	0.86	205.1	0.010	126.42	26.7
Sum	4156	100						
Average weighted by land use						0.0125	195.1	12.53
Uniform model run						0.0155	44.0	5.70

and 1410 for the spatially variable model run. Table 2 provides an overview of the values of K_{sat}, Manning's *n*, and *k* as provided in the GCTE data set and, following calibration, as used in Cascade 6 for the various land use classes for the event of 26 June 1987. Table 2 also shows the values of the uniform or effective parameters (Blöschl & Sivapalan, 1995), derived using a separate calibration.

Based on the % area for the various land use classes, areally weighted average values of K_{sat}, Manning's *n*, and *k* were calculated. Comparison with the values of K_{sat}, Manning's *n*, and *k* based on calibration of Cascade 6 for peak discharge and sediment rating curve for the uniform parameter run shows a close similarity for Manning's *n* (0.0125 for the areally weighted average *vs* 0.0155 for the uniform case), but large differences for the K_{sat} (12.53 mm h^{-1} for the areally weighted average *vs* 5.70 mm h^{-1} for the uniform case) and *k* (195.1 for the areally weighted average *vs* 44.0 for the uniform case). The substantial difference for K_{sat} and *k* shows that applying areally averaged parameter values to the entire basin will provide a model result that is different from that obtained using uniform parameters determined through a separate calibration. This result indicates that the model basin responds non-linearly to changes in the spatial pattern of the input parameters, and suggests that the spatial pattern of input parameter values is an important feature controlling basin response.

The map of the land use classes (Fig. 2(a)) and associated parameter values (Table 2) indicate that the rate of runoff generation differs substantially within the basin. For example, land use class 4 with K_{sat} = 3.3 mm h^{-1} will, under uniform rainfall conditions, generate much more runoff than land use classes 5, 6, 14 and 15 with K_{sat} = 26.7 mm h^{-1}. For this particular event, the differences in runoff generation between the various land use classes can be expected to result in differences in erosion rate because the *k* factor is very similar for the different land use classes: 147 for land use class 4 and 126.42 and 149.94 for land use classes 5, 6, 14 and 15 (Table 2). In an area of uniform land use, and uniform runoff and erosion parameters, such as in the southeastern portion of the basin which is all under land use 4, a map of erosion rates for the model run with spatially variable parameters shows a well defined spatial pattern defined by topography (Fig. 2(b)), with erosion on the ridges and deposition on the lower parts of the slopes (Fig. 3(a)). Conversely, in an area with varied land use,

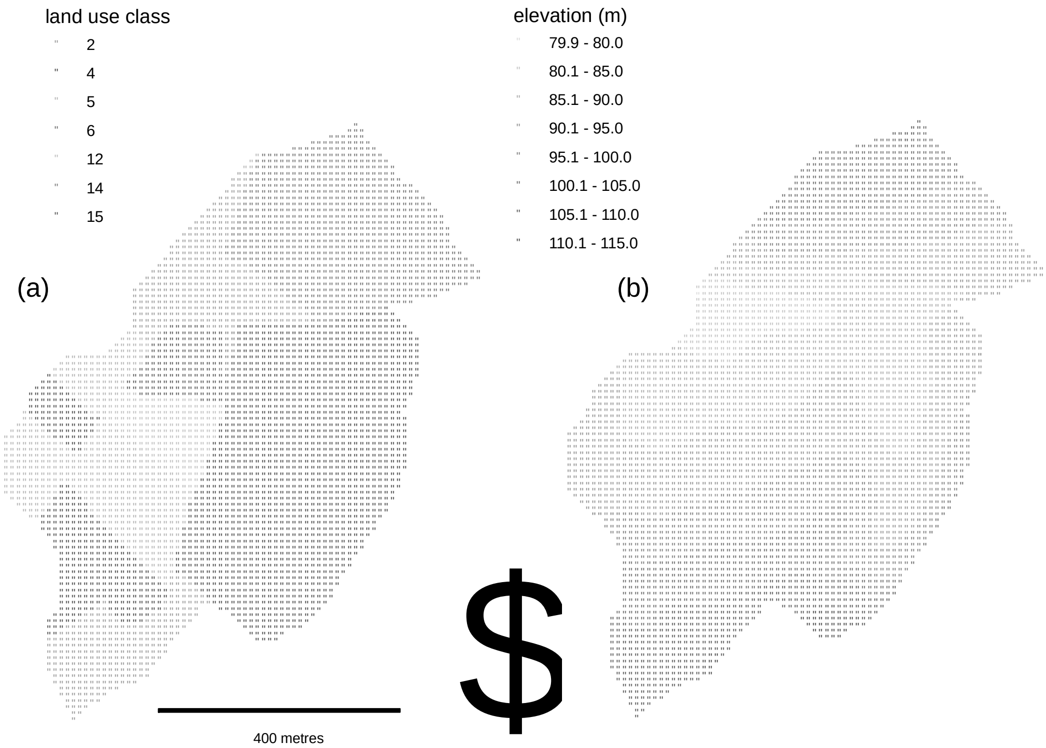

Fig. 2 Land use (a) and topography (b) in the Catsop basin.

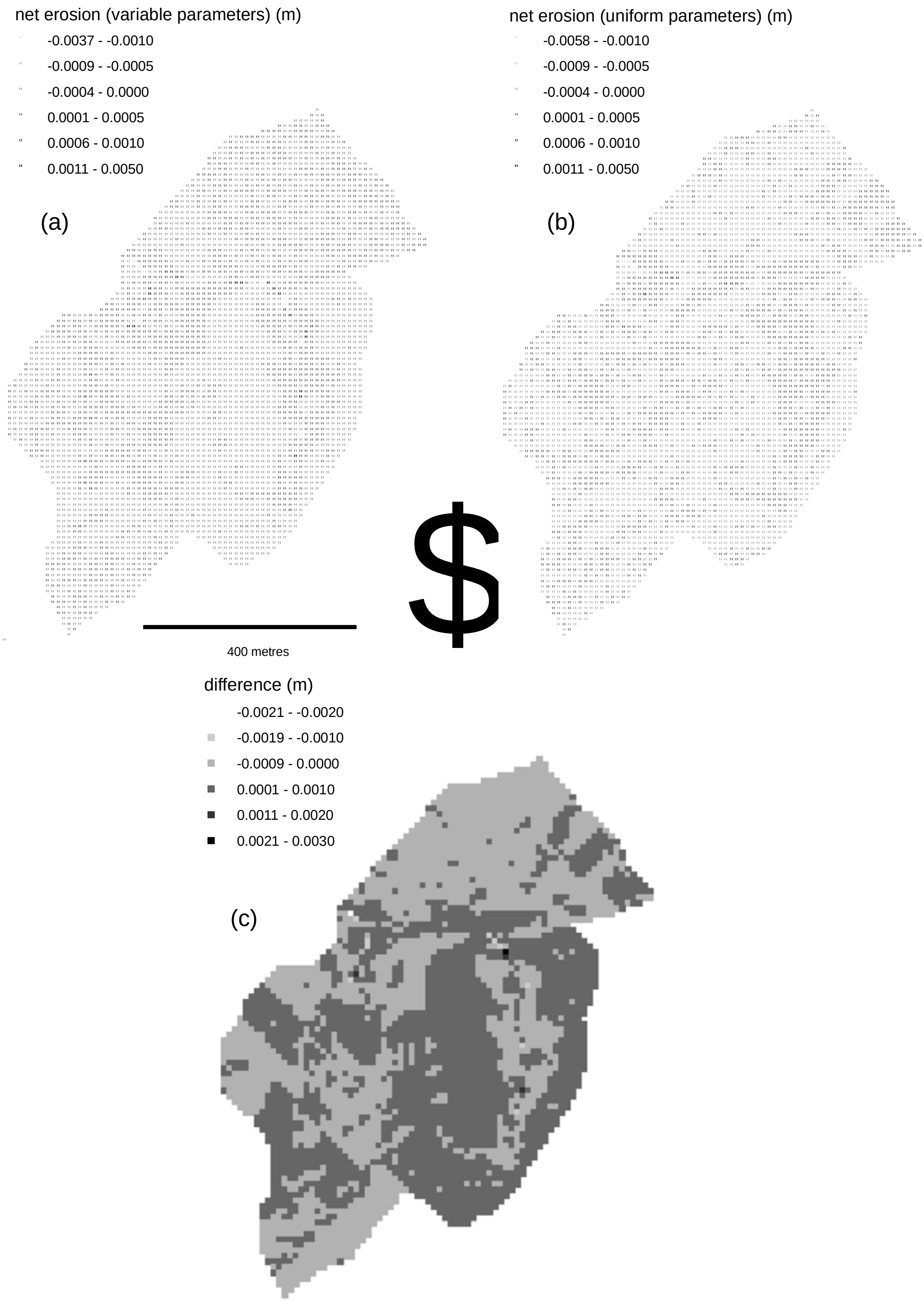

Fig. 3 Erosion pattern for the 870626 event modelled with spatially variable (a) and uniform (b) parameters, and the difference in modelled erosion (c). Negative values in the map of differences (c) indicate that erosion calculated with variable parameters is greater; positive values indicate that erosion calculated with uniform parameters is greater.

such as in the southwestern portion of the basin, the erosion pattern reflects land use in combination with topography. For example, land use classes 4 and 12 show predominantly erosion, whereas land use classes 2 and 5 show a mix of erosion and deposition, as does land use class 6 in the northern part of the basin. Within every land use class, however, some cells show erosion and other deposition, and land use class cannot be used to predict erosion rate.

The erosion pattern obtained with uniform runoff and erosion parameters shows some of the features of the erosion pattern computed with variable parameters (Fig. 3(b)). Of course, the different land use classes are not expressed in the erosion pattern because the parameters are uniform. The effect of topography, however, is clearly visible, for example in the southeastern part of the basin, where erosion, indicated by negative values, is found on the ridges and deposition, indicated by positive values, occurs lower on the slopes. In other parts of the basin consisting predominantly of long, straight slopes such as in the southwestern and northern parts of the basin, the erosion pattern is not well defined. A comparison of the two erosion patterns (Fig. 3(c)) shown as the difference between the patterns indicates that, in the southeastern part of the basin, total erosion and total deposition computed with variable parameters exceeds that computed with uniform parameters on the ridges and the lower slopes, respectively. In the southwestern part of the basin, the difference between the erosion patterns predominantly reflects the land use pattern. For example, on land use classes 4 and 12, the difference between the erosion patterns is predominantly positive meaning that the total erosion computed with variable parameters exceeds that computed with uniform parameters. This is explained by a combination of lower values of K_{sat} (3.3) and higher values of k (147) for this land use class compared to the uniform case for which K_{sat} = 5.70 and k = 44, resulting in more runoff and erosion.

A plot of net erosion modelled with variable and with uniform parameters shows a linear relationship between the erosion rates (Fig. 4). If the grid cells are classified based on drainage area, calculated from the number of cells contributing runoff and sediment to a cell, the line of best fit is described by the following equations:

For cells with a drainage area <100 m^2 (13.8% of basin area):

$$y = 1.8939x - 2 \times 10^{-6} \ (r^2 = 0.4684) \qquad (2a)$$

For cells with a drainage area between 100 and 100 000 m^2 (85.1% of the basin area):

$$y = 3.755x + 1 \times 10^{-6} \ (r^2 = 0.7297) \qquad (2b)$$

For cells with a drainage area greater than 100 000 m^2 (1.1 % of the basin area):

$$y = 0.8063x + 0.0002 \ (r^2 = 0.7978) \qquad (2c)$$

where x is net erosion in a grid cell computed with uniform parameters and y is total erosion computed with variable parameters. Equation (2) indicates that the total erosion and deposition computed with variable parameters is greater than that computed using uniform parameters for drainage areas up to 100 000 m^2. For cells with a larger drainage area, associated with the channel system, this relationship is reversed.

Equation (2b) enables the prediction of erosion for variable runoff and erosion parameters from the erosion modelled with the effective parameters. Figure 5 shows the difference between erosion predicted using equation (2) and modelled using Cascade 6 with variable parameters. As expected, the pattern reflects both land use, mostly on the

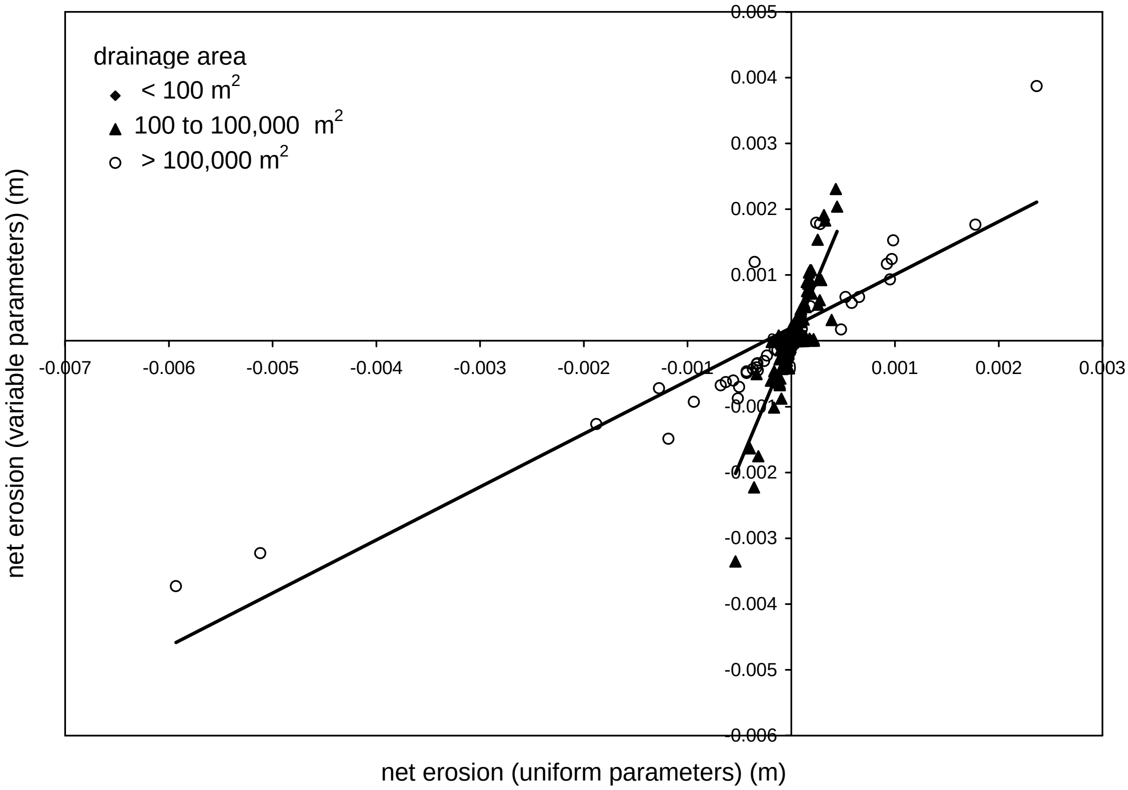

Fig. 4 Net erosion for individual cells modelled with uniform parameters and spatially variable parameters for drainage areas <100 m^2, 100 to 100 000 m^2, and >100 000 m^2.

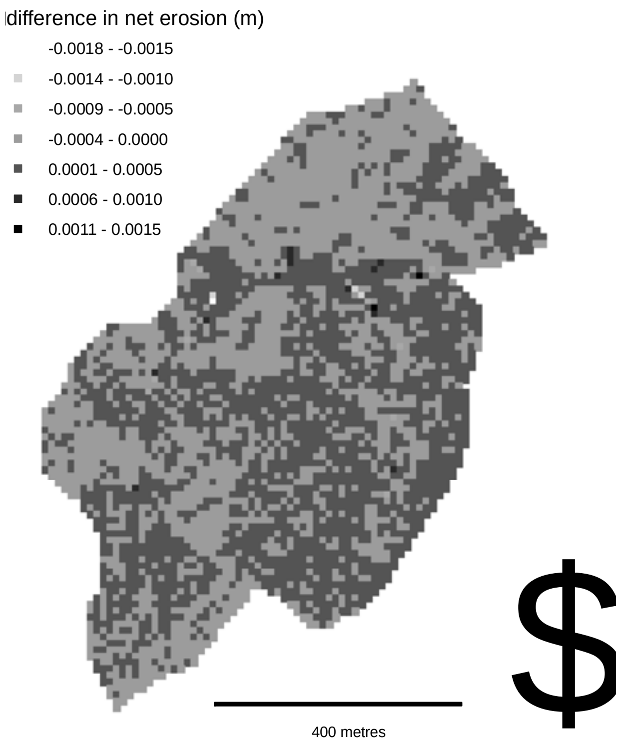

Fig. 5 Difference between erosion predicted using Cascade 6 with uniform parameters and equation (2), and modelled using Cascade 6 with variable parameters.

west side, and topography, mostly on the east side of the basin. Table 3 shows for the various land use classes the average difference between the erosion predicted using equation (2) and modelled using Cascade 6 with variable parameters for grid cells with a drainage area between 100 and 100 000 m^2. As expected, the difference varies between land use classes, depending primarily on the value of K_{sat}. For land use classes 5, 6, 14 and 15, the magnitude of erosion predicted with equation (2) exceeds the magnitude predicted with Cascade 6 with variable parameters, whereas for land use classes 2, 4 and 12 the situation is reversed. The difference in magnitude of predicted erosion can be explained by the difference in K_{sat} for the various land use types. For land use classes 5, 6, 14 and 15, K_{sat} is less than 5.70 mm h^{-1}, the value used as the effective parameter. This results in the generation of more overland flow on these land use classes, and consequently more erosion. Conversely, for land use classes 2, 4 and 12, K_{sat} is similar in magnitude to the value used as effective parameters, resulting in similar amounts of runoff and erosion.

Table 3 Average difference between erosion predicted using regression and Cascade 6 with variable parameters.

Land-use class	Average difference in predicted erosion
2	6.4125E-06
4	4.21907E-06
5	–1.04089E-05
6	–5.57075E-06
12	1.09177E-06
14	–1.55771E-05
15	–1.26833E-05

CONCLUSIONS

Notwithstanding the importance of land use for explaining erosion patterns, in many drainage basins detailed information about land use patterns and the runoff and erosion parameters associated with different types of land use is just not available. To overcome this deficiency, erosion models can be run using effective runoff and erosion parameters, and the modelling results can then be treated to approximate the results that would have been obtained using variable parameters. In the case of the Catsop basin modelled with Cascade 6, it was found that regression equations could be used to derive the erosion pattern modelled with variable parameters from the erosion pattern modelled using effective parameters for cells with a drainage area between 100 and 100 000 m^2. For cells with a drainage area smaller than 100 m^2, the regression equation explained only 47% of the variance.

Acknowledgements The author gratefully acknowledges: the hospitality of Coen Ritsema and his Land Use and Soil Processes research group of Alterra at Wageningen University; the comments and insights provided by Victor Jetten; and a sabbatical leave travel grant from the University of Saskatchewan.

REFERENCES

Blöschl, G. & Sivapalan, M. (1995) Scale issues in hydrological modelling: a review. *Hydrol. Processes* **9**, 251–290.

De Boer, D. H. (2001) Self-organization in fluvial landscapes: sediment dynamics as an emergent property. *Computers & Geosci.* **27**, 995–1003.

De Boer, D. H. (2005) Predicting sediment rating curves with a cellular landscape model. In: *Sediment Budgets 2* (ed. by A. J. Horowitz & D. E. Walling) (Proc. Foz do Iguaçu Symp., April 2005), 75–84. IAHS Publ. 292. IAHS Press, Wallingford, UK.

De Boer, D. H. & Ali, K. F. (2002) Sediment budgets and self-organization in a cellular landscape model. In: *The Structure, Function and Management Implications of Fluvial Sedimentary Systems* (ed. by F. J. Dyer, M. C. Thoms & J. M. Olley) (Proc. Alice Springs Symp., September 2002), 365–372. IAHS Publ. 276. IAHS Press, Wallingford, UK.

De Roo, A. P. J. (1996) The LISEM project: an introduction. *Hydrol. Processes* **10**, 1021–1025.

De Roo, A. P. J. (1998) Modelling runoff and sediment transport in catchments using GIS. *Hydrol. Processes* **12**, 905–922.

De Roo, A. P. J. & Jetten, V. G. (1999) Calibrating and validating the LISEM model for two data sets from the Netherlands and South Africa. *Catena* **37**, 477–493.

De Roo, A. P. J., Wesseling, C. G. & Ritsema, C. J. (1996a) LISEM: a single event physically-based hydrologic and soil erosion model for drainage basins: I. Theory, input and output. *Hydrol. Processes* **10**, 1107–1117.

De Roo, A. P. J., Offermans, R. J. E. & Cremers, N. H. D. T. (1996b) LISEM: a single event physically-based hydrologic and soil erosion model for drainage basins: II. Sensitivity analysis, validation and application. *Hydrol. Processes* **10**, 1119–1126.

Dietrich, W. E., Bellugi, D. G., Sklar, L. S., Stock, J. D., Heimsath, A. M. & Roering, J. J. (2003) Geomorphic transport laws for predicting landscape form and dynamics. In: *Prediction in Geomorphology* (ed. by P. R. Wilcock & R. M. Iverson), 103–132. Geophysical Monograph 135. American Geophysical Union, Washington, DC, USA.

Favis-Mortlock, D. & De Boer, D. H. (2003) Simple at heart? Landscape as a self-organizing complex system. In: *Contemporary Meanings in Physical Geography* (ed. by S. T. Trudgill, A. Roy & A. Kirkbride), 127–171. Arnold, London, UK.

Howard, A. D. (1994) A detachment-limited model of drainage basin evolution. *Water Resour. Res.* **30,** 2261–2285.

Jetten, V., De Roo, A. & Favis-Mortlock, D. (1999) Evaluation of field-scale and catchment-scale soil erosion models. *Catena* **37**, 521–541.

Jetten, V, Govers, G, & Hessel, R. (2003) Erosion models: quality of spatial predictions. *Hydrol. Processes* **17,** 887–900.

Kirkby, M. J. (1993) Long term interactions between networks and hillslopes. In: *Channel Network Hydrology* (ed. by K. Beven & M. J. Kirkby), 255–294. Wiley, Chichester, UK.

Tucker, G. E. & Slingerland, R. (1997) Drainage basin responses to climate change. *Water Resour. Res.* **33**, 2031–2047.